Effects of Titration Parameters on the Synthesis of Molybdenum Oxides Based Catalyst
(Kesan Parameter Penitratan terhadap Sintesis Mangkin Molibdenum Oksida)

D.D. Suppiah*, F.A. Hamid, M.G. Kutty & S.B. Abd Hamid

ABSTRACT

Molybdenum oxides catalysts are extensively used in various selective oxidation reactions. In this work, controlled precipitation method was used to synthesise molybdenum oxides. The effects of various titration parameters on the precipitate growth rate and structure throughout catalyst synthesis were investigated. The titration parameters varied for this study were molybdates (ammonium heptamolybdate) concentration, precipitation agent (HNO_3) concentration, precipitating agent rate of addition and temperature of synthesis. X-Ray diffraction (XRD) and Field Emission Scanning Electron Microscope (FESEM) were used to characterize the catalysts. This study highlights the significant effects of the titration parameters varied on the supersaturation of the solution therefore yielding precipitate with different morphology. It was observed that the temperature played the major role followed by molybdate concentration in the formation of the bulk catalyst. Supramolecular structure ($Mo_{36}O_{112}$) was observed at lower temperature (30ºC) and lower molybdate concentration (0.07 M, 0.10 M) while at higher temperature (50ºC) and higher molybdate concentration(0.14 M) hexagonal (h-MoO_3) phase structure was formed. Fast rate of addition and high concentration of precipitating agent affected the solution equilibrium leading to unclear inflection point (supersaturation point) at the titration curve.

Keywords: Catalyst; molybdenum oxides; precipitation; titration

ABSTRAK

Mangkin molibdenum oksida digunakan secara meluas dalam pelbagai tindak balas pengoksidaan terpilih. Kaedah pemendapan yang terkawal telah digunakan dan pelbagai parameter penitratan telah digunakan seperti kepekatan molibdat (ammonia heptamolybdate), kepekatan agen pemendapan (HNO_3), kadar penambahan agen pemendapan dan suhu sintesis. Kesan setiap parameter terhadap kadar pertumbuhan dan struktur zarah semasa sintesis mangkin telah dikaji. Pembelauan sinar-X (XRD) dan Mikroskop Pancaran Medan Elektron Imbasan (FESEM) digunakan untuk mengenal pasti ciri-ciri mangkin. Berdasarkan kajian yang telah dibuat, perkara utama yang perlu diberi perhatian adalah kesan setiap parameter penitratan terhadap keterlarutan yang menghasilkan pemendapan pepejal dengan morfologi berbeza. Suhu memainkan peranan paling penting diikuti kepekatan molibdat dalam pembentukan mangkin pukal. Struktur supramolekular ($Mo_{36}O_{112}$) telah diperhatikan pada suhu rendah (30ºC) dan kepekatan molibdat rendah (0.07 M, 0.10 M) sedangkan pada suhu tinggi (50ºC) dan kepekatan molibdat tinggi (0.14 M) struktur hexagonal (h-MoO_3) telah dihasilkan. Kadar penambahan yang cepat dan kepekatan tinggi agen penitratan mempengaruhi keseimbangan larutan dan mengakibatkan titik keterlarutan yang tak jelas.

Kata kunci: Mangkin; molibdenum oksida; pemendapan; penitratan

INTRODUCTION

Molybdenum oxides (MoO_x) have been widely studied as a selective oxidation catalyst in various reactions such as oxydehydrogenation, isomerization and hydrogenation of light olefins (C_2-C_4) (Chang et al. 2002; Haddad et al. 2009). Molybdenum oxides exhibit ample structural intricacy and this criterion has been shown to contribute to catalytic activity (Cavalleri et al. 2007; Dieterle et al. 2001). The main strategies adapted when synthesizing MoO_x focus on controlling growth of the particles and self-organization of the polyoxometalates (Cronin et al. 2000; Dillon et al. 2003). Hydrothermal process has been extensively used to synthesis MoO_x catalyst but the process is time consuming and requires high temperature. These drawbacks make it difficult to control and attain the desired crystal structure, elemental composition, particle shape, surface area and other properties (Song et al. 2007; Ueda et al. 2008; Wang et al. 2005).

Controlled precipitation method allows particles with not only different morphology to be obtained but also ensures the reproducibility of the synthesized material (Rodriquez-Paez et al. 2001). This is based on the control of parameters such as temperature, pH, reactant concentration and time which are correlated with factors such as supersaturation, nucleation and growth rates, surface energy and diffusion coefficients of the precipitate (Yu et al. 2007). Abd Hamid et al. (2003) and Wagner et al. (2004) have identified that precipitation parameters such

as temperature, rate of precipitating agent addition and molybdates concentration influences the structural complex of MoO_x (Abd Hamid et al. 2003; Wagner et al. 2004). However, a thorough study on the influence of titration parameters in the structural formation of the molybdenum oxide catalyst is lacking. In this paper, we investigated the role of the titration parameters of the precipitation method in determining the composition and structure of the final product. Detailed understanding of these conditions will allow for better control of the desired output product and allow for the process to be optimized.

MATERIALS AND METHODS

CATALYST PREPARATION

The synthesis method used in this work follows the technique established by Abd Hamid et al. (2003). In this study, the method is further optimized by adding more variations to the controlled parameters. Molybdenum oxides (MoO_x) precursors were synthesized via controlled precipitation method. Ammonium heptamolybdate (AHM) was used as the molybdate source and nitric acid (HNO_3) was used as the precipitating agent. Parameters varied were temperature (30°C and 50°C), molybdate solution concentration (0.07 M, 0.10 M and 0.14 M), precipitating agent concentration (1 M, 2 M and 5 M) and rate of addition (1 mL/min, 3 mL/min and 5 mL/min). This was done to establish a set of relationship between the parameters and investigate the effects of each variable on the molybdenum oxide structure. The various matrix of experiments with varying parameters is shown in Table 1. The balanced equation for the reaction is shown below. The acid was added to the AHM solution with a fine control of the rate of addition using an autotitrator (Mettler Toledo DL50). The solution was concurrently stirred at desired temperature on a hot plate and the pH changes were monitored throughout the titration process and termination point was set at pH 1.

$$(NH_4)_6[Mo_7O_{24}]+6H^+ \rightarrow 7\ MoO_3 + 6NH_4^+ + 3H_2O \tag{1}$$
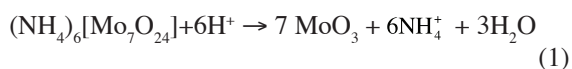
All precipitate obtained were vacuum filtered using a Buchner flask and vacuum pump at -20 bar. The precipitates were then dried using vacuum dessicator for 3 days at 30°C.

CATALYST CHARACTERIZATION

The synthesized catalyst precursors were subjected to structural analysis using Bruker's powder x-ray diffractometer (XRD). The data sets were collected in reflection geometry in the range of $2° \leq 2\theta \leq 60°$ with a step size of $\Delta 2\theta = 0.02°$ Phase analysis was done by matching the data with the ICDD library and phase purity was determined using EVA software (Version 2002). The average crystallite sizes of the synthesized of MoO_x were calculated from the full-width at half maximum (FWHM) of the XRD main peak broadening using Scherrer equation.

FEI quanta 200F Field Emission Scanning Electron Microscope (FESEM) was used to evaluate the particle size and morphology of the catalyst. The micrographs were taken under low vacuum and accelerating voltage of 5.0 HV.

RESULTS AND DISCUSSION

EFFECTS OF TEMPERATURE

Table 1 shows a summary of the samples synthesized and their experimental conditions. The effect of varying temperature of the AHM solution was investigated by looking at samples M033 and M039. The samples were synthesized at 30ºC (M033) and 50ºC (M039) while maintaining all other parameters as a constant. Figure 2 shows the titration curve and pH first derivatives comparison for M033 and M039. Based on the titration curve for M039, the starting pH was lower, implying that heating the AHM solution increases the solubility and dissociation of AHM in water giving rise to H^+ ions, thus increasing acidity (Zhang et al. 2011). Based on the first derivative curve, M033 exhibits 2 inflection points. At the first minimum point, no obvious precipitate was observed but a cloudy suspension was noticed. However, at the maximum inflection point, spontaneous white precipitate was observed. Figure 1 shows the XRD patterns of all synthesized samples. The XRD diffractogram for M033 exhibits the general 'supramolecular' structure ($Mo_{36}O_{112}$) properties where high intensity peaks are observed at 2θ lower angle (7°) and peaks are roughly resolved with low

TABLE 1. MoO_x precursors synthesized using various conditions

Sample No	$[MoO_4]^{2-}$ (Mol/l)	Temperature (°C)	$[H]^+$ Mol/l	Rate of addition (mL/min)
M033	0.10	30	1	1
M064	0.10	30	1	3
M065	0.10	30	1	5
M014	0.07	30	1	1
M035	0.14	30	1	1
M043	0.10	30	2	1
M021	0.10	30	5	1
M039	0.10	50	1	1

intensity at higher diffraction angle (10°-12°). The lower intensity peaks observed at higher angle indicates the ordering of polyoxymolybdate nanostructured building blocks (Abd Hamid et al. 2003). The building blocks consisting of MoO_7 units were formed at the first inflection point. As shown in Table 2, the crystallite size of M033 was about 14.1 nm. As protonation continues, particles nucleation takes place as solution supersaturation was reached. The bridging of oxygen atoms networks of the MoO_7 leads to the nuclei growth and assembles into a new bulk material of polyoxymolybdate (Cronin et al. 2000; Hu & Shaw 1999).

M039 titration curve did not exhibit a maximum point as compared to M033. When heated, the solution supersaturation decreases as MoO_7 particles solubility was increased in the solution and therefore no spontaneous precipitation was observed (Feng et al. 2007). Significantly lesser amount of acid was needed for M039 synthesis to reach the end point. This coincides with the increase of

proton consumption when temperature was raised (Duc et al. 2008). The titrated solution was then further heated to 70°C and fine white precipitates were observed. The XRD diffractogram obtained for M039 have hexagonal phase properties and corresponds to the compound ammonium molybdenum oxide hydrate, $(NH4)_{0.15}MoO_3.0.5H_2O$ (PDF-File 29-0115). This was because temperature changes the MoO_7 solubility which then affects the morphology of the structure (Feng et al. 2007). The crystallite size of M039 calculated was about 13.0 nm which was smaller than M033. There is a small peak shift suggesting stacking faults due to internal stress and this can be seen in the SEM images in Figure 6(d) (Ungar 2004).

Figures 6(a) and 6(b) show the SEM images for M033. The image shows large fraction of needle-like agglomerates (Wagner et al. 2004). At higher magnification, it is observed that there are long blocks with no particular shape. The SEM images of M039 as displayed in Figures 6(c) and 6(d) shows clear hexagonal structure further confirming the XRD
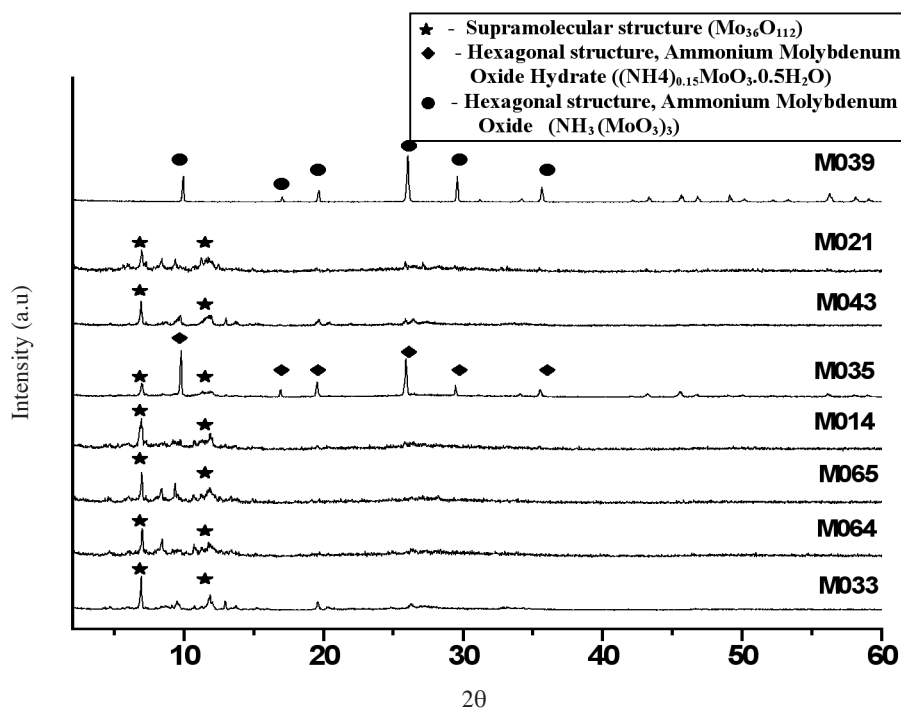

FIGURE 1. XRD patterns of synthesized samples

TABLE 2. MoO_x major phases and the crystallite sizes

Sample No	Major phases	Crystallite sizes
M033	Supramolecular	14.1
M064	Supramolecular	12.8
M065	Supramolecular	14.8
M014	Supramolecular	6.1
M035	Hexagonal	12.2
M043	Supramolecular	11.2
M021	Supramolecular	8.6
M039	Hexagonal	13.0

analysis. The lower magnification image shows a cluster of the long rods with hexagonal cross section (Song et al. 2007).

Effects of Molybdate Concentration. The second experiment was conducted by varying the AHM concentration. Figure 3 shows the titration curve and pH first derivatives comparison of samples M014, M033 and M035 with AHM concentrations of 0.07, 0.10 and 0.14, respectively. Similar pattern of titration curve was observed for all three samples. The minimum point of the derivative curve gradually shifts as the concentration increases since more acid is needed to reach the buffering equilibrium. The XRD patterns of M014, M033 and M035 are shown in Figure 1. Diffractograms of samples synthesized at higher concentration of AHM (0.10 M and 0.14 M) exhibits the supramolecular phase properties. However, the intensity of the prominent peak at 2θ of 7° was varied indicating a boost of oxygen influence on the structure (Bohne et al. 2005). The crystallite size of M014 which is shown in Table 2, was smaller as compared to M033. The crystallinity of the molybdenum oxide particles increases with concentration, hence larger crystallite size (Mahajan et al. 2008).

Two minimum points in the titration curve were observed for M035 indicating heterogeneous nucleation

process takes place at different pH. The unstable colloidal distribution of the precipitate consisting of MoO_x species cannot be maintained and the crystallite fragment interlinks and progressively grew forming larger units (Chow & Kurihara 2002). When supersaturation was reached, the white precipitate obtained was made out of polyoxymolybdate bulk structure. This has been confirmed by the XRD diffractograms obtained which also matches the hexagonal phase however corresponds to the compound ammonium molybdenum oxide, $NH_3(MoO_3)_3$ (PDF-File 78-1027). However, there are relatively low intensity unmatched peaks, suggesting phase mixture with supramolecular structure as these peaks were at 2θ of 7° and at 10°-12°. This shows molybdate concentration does influence phase structure of molybdenum oxide.

As shown in Table 2, the average crystallite size comparison for both hexagonal structures of M035 and M039 appears to be similar. Figures 6(e) and 6(f) show the SEM images for M035. The XRD analysis implies a phase mixture of supramolecular structure and hexagonal. At lower magnification, the agglomerates are like long blocks with no particular shape similar to the supramolecular structure in Figure 6(a) but at higher magnification the hexagonal cross section of the rods are clearly seen which is larger than M025. This is in good agreement with the
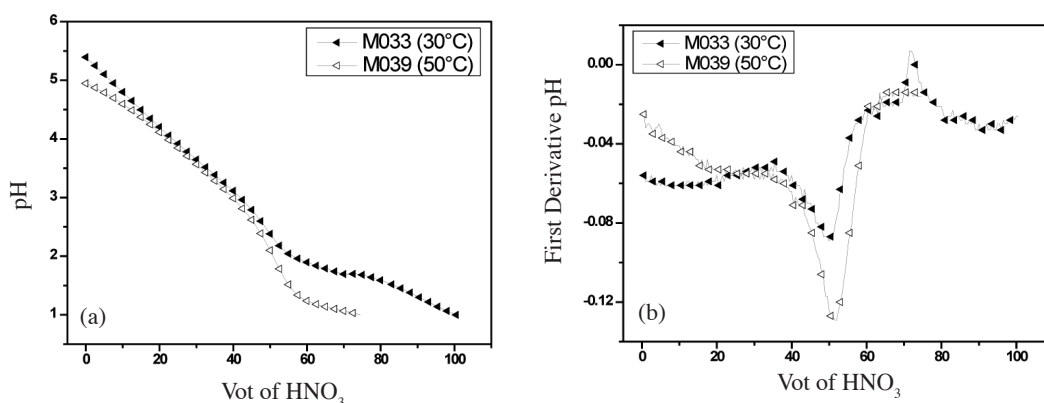

FIGURE 2. Titration of 0.10 M AHM with 1.0 M HNO$_3$ at different temperature for (a) pH and (b) pH first derivative
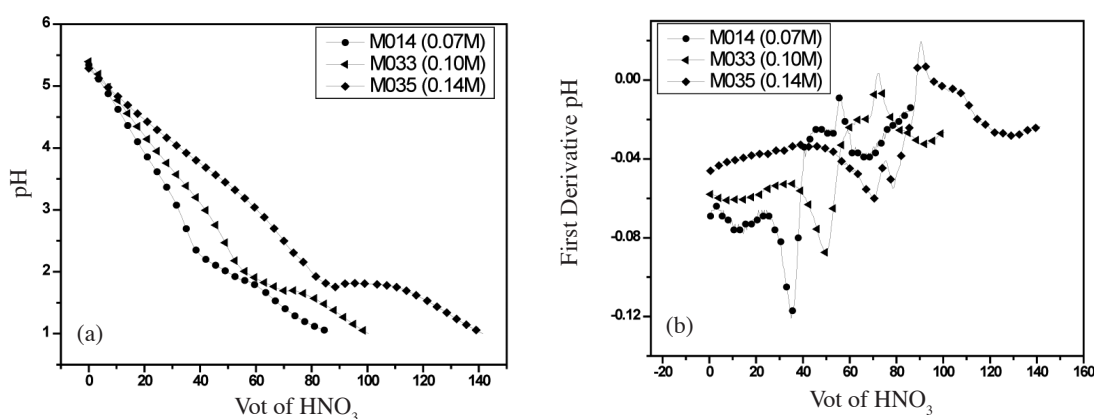

FIGURE 3. Titration of AHM at different concentration with 1.0 M HNO$_3$ at 1mL/min for (a) pH and (b) pH first derivative
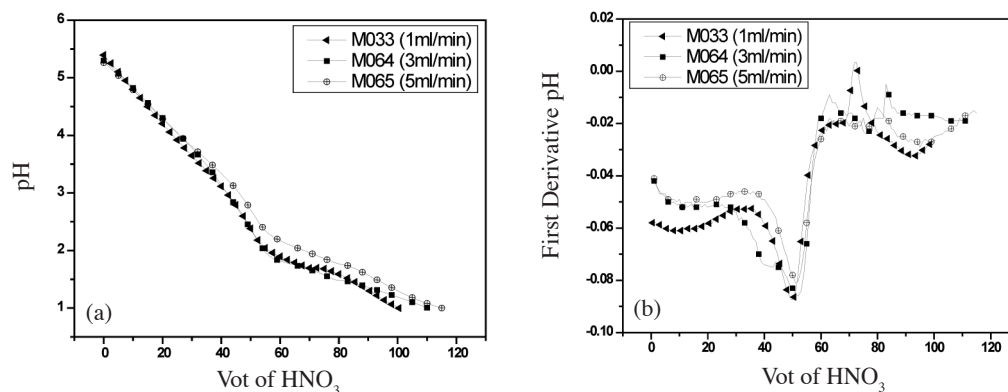
FIGURE 4. Titration curve and derivative of 0.10M AHM with 1.0 M HNO_3
at different rate of addition for (a) pH and (b) pH first derivative
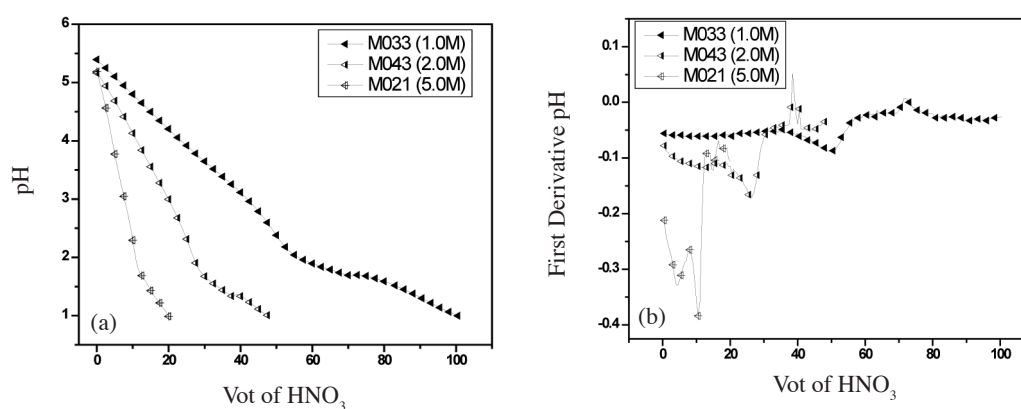

FIGURE 5. Titration of 0.10 M AHM with HNO_3 at different concentration for
(a) pH and (b) pH first derivative

influence of supersaturation on the morphology of the precipitate. At lower supersaturation, the particles formed are small and nicely shaped while at higher supersaturation level larger particles are formed (Chow & Kurihara 2002; Yu et al. 2007).

Effects of Rate of Addition. The third controlled precipitation experiment was conducted by varying the rate of addition of the precipitating agent (HNO_3). Figure 4 shows the titration curve and pH first derivatives comparison for M033, M064 and M065 with titration rate of 1 mL/min, 3 mL/min and 5 mL/min, respectively. All three pH first derivatives curves exhibit one minimum point and one maximum point. Almost the same amount of acid is needed to reach the first inflection point for all three curves. The pH curves become less steeper indicating that the continuous addition of acid is consumed for the precipitation therefore contributes lesser to the pH changes (Behrens et al. 2011). The maximum inflection point however differs for all curves. Buffering equilibrium is not reached during fast addition (5mL/min) resulting in delay of reaction sequence. Therefore, M065 has the smallest maximum point followed by M064 and M033 (Abd Hamid et al. 2003). The average crystallite

size of all three synthesized sample were 14.1 nm, 12.8 nm and 14.8 nm. These values are very similar to each other suggesting the rate of precipitating agent addition does not influence greatly on the crystallite size of the molybdenum oxide particles.

Effects of Precipitating Agent (HNO_3) Concentration. The last experiment was conducted by varying the precipitating agent concentration which in this experiment is HNO_3. Figure 5 shows the titration curve and pH first derivatives comparison of M033, M043 and M021. The higher the concentration of HNO_3 used, the lesser amount of acid was needed to reach the termination point. Based on the derivatives, sharp pH change causing huge error in the curve was observed for M021 leading to inflection point uncertainty. However, for titration using lower acid concentration, small but unambiguous pH change is observed.

CONCLUSION

Solution supersaturation, which can be observed from the titration curves, was mainly affected by temperature. At 30ºC, precipitate formed exhibit polyoxymolybdate
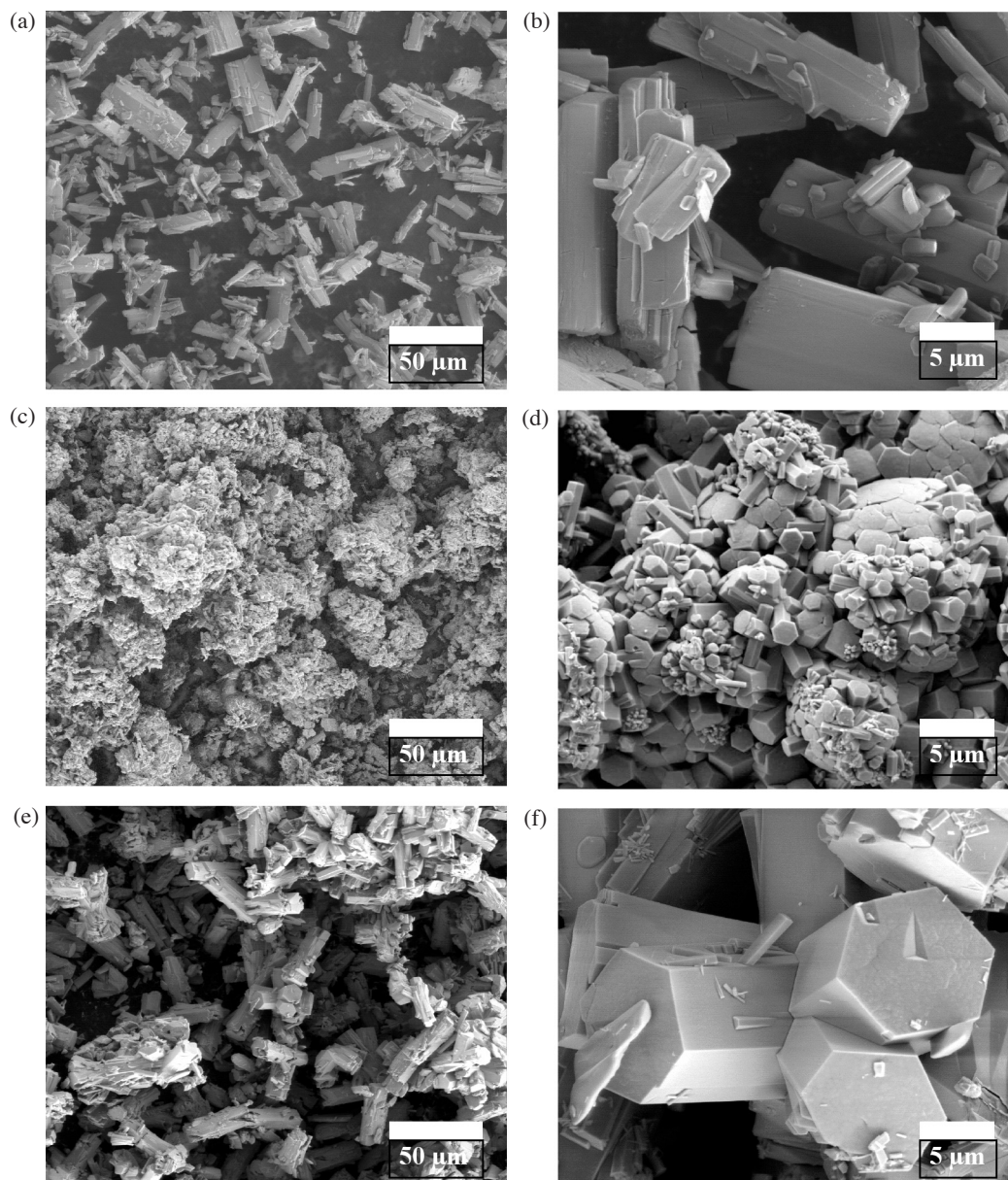
(a)

(b)

(c)

(d)

(e)

(f)

FIGURE 6. SEM imaging of M033 (a,b), M025 (c,d) and M035 (e,f)

supramolecular structure ($Mo_{36}O_{112}$) properties. At 50ºC, no spontaneous precipitation was observed and by further heating to higher temperature, solution supersaturation was reached and the precipitate displays hexagonal phase structure (h-MoO_x). Molybdate concentration also affects the structural formation where at lower concentration (0.07 M, 0.10M), supramolecular structure was obtained while at higher concentration (0.14 M), hexagonal structure was obtained. Rate of addition affects the buffering equilibria where at faster rate (5 mL/min) the supersaturation point was undefined, hence unable to acquire pure phase materials. The same drawbacks are seen using high HNO_3 concentration (5 M). By using all the information obtained from the titration effects, desired and pure phase reproducible bulk catalysts can be synthesized.

REFERENCES

Abd Hamid, S.B., Othman, D., Abdullah, N., Timpe, O., Knobl, S., Niemeyer, D., Wagner, J., Su, D. & Schogl, R. 2003. Structurally complex molybdenum oxide model catalysts for the selective oxidation of propene. *Topics in Catalysis* 24(1): 87-95.

Behrens, M., Brennecke, D., Girgsdies, F., Kißner, S., Trunschke, A., Nasrudin, N., Zakaria, S., Idris, N.F., Hamid, S.B.A., Kniep, B., Fischer, R., Busser, W., Muhler, M. & Schlögl, R. 2011. Understanding the complexity of a catalyst synthesis:

Co-precipitation of mixed Cu,Zn,Al hydroxycarbonate precursors for Cu/ZnO/Al$_2$O$_3$ catalysts investigated by titration experiments. *Applied Catalysis A: General* 392(1-2): 93-102.

Bohne, Y., Shevchenko, N., Prokert, F., von Borany, J., Rauschenbach, B. & Möller, W. 2005. In situ characterization of phase formation during high-energy oxygen ion implantation in molybdenum. *Nuclear Instruments and Methods in Physics Research Section B: Beam Interactions with Materials and Atoms* 240(1-2): 157-161.

Cavalleri, M., Hermann, K., Guimond, S., Romanyshyn, Y., Kuhlenbeck, H. & Freund, H.J. 2007. X-ray spectroscopic fingerprints of reactive oxygen sites at the MoO$_3$(0 1 0) surface. *Catalysis Today* 124(1-2): 21-27.

Chang, Z., Song, Z., Liu, G., Rodriguez, J.A. & Hrbek, J. 2002. Synthesis, electronic and chemical properties of MoO$_x$ clusters on Au(1 1 1). *Surface Science* 512(1-2): L353-L360.

Chow, G. & Kurihara, L.K. 2002. Chemical synthesis and processing of nanosructured powders and films. In: Koch, C.C. (ed). *Nanostructured materials processing, properties and potential*. New York: William Andrew Publishing pp. 3-50.

Cronin, L., Kögerler, P. & Müller, A. 2000. Controlling growth of novel solid-state materials via discrete molybdenum-oxide-based building blocks as synthons. *Journal of Solid State Chemistry* 152(1): 57-67.

Dieterle, M., Mestl, G., Jäger, J., Uchida, Y., Hibst, H. & Schlögl, R. 2001. Mixed molybdenum oxide based partial oxidation catalyst: 2. Combined X-ray diffraction, electron microscopy and Raman investigation of the phase stability of (MoVW)$_5$O$_{14}$-type oxides. *Journal of Molecular Catalysis A: Chemical* 174(1-2): 169-185.

Dillon, C.J., Holles, J.H., Davis, R.J., Labinger, J.A. & Davis, M.E. 2003. A substrate-versatile catalyst for the selective oxidation of light alkanes: II. Catalyst characterization. *Journal of Catalysis* 218(1): 54-66.

Duc, M., Carteret, C., Thomas, F., & Gaboriaud, F. 2008. Temperature effect on the acid-base behaviour of Na-montmorillonite. *Journal of Colloid and Interface Science* 327(2): 472-476.

Feng, B., Yong, A.K. & An, H. 2007. Effect of various factors on the particle size of calcium carbonate formed in a precipitation process. *Materials Science and Engineering: A* 445-446(0): 170-179.

Haddad, N., Bordes-Richard, E. & Barama, A. 2009. MoO$_x$-based catalysts for the oxidative dehydrogenation (ODH) of ethane to ethylene: Influence of vanadium and phosphorus on physicochemical and catalytic properties. *Catalysis Today* 142(3-4): 215-219.

Hu, E.L. & Shaw, D.T. 1999. Synthesis and Assembly. In: R.W. Siegel, Hu, E. and Roco, M.C. (ed). *Nanostructure Science and Technology A Worldwide Study* pp. 15-34.

Mahajan, S.S., Mujawar, S.H., Shinde, P.S., Inamdar, A.I. & Patil, P.S. 2008. Concentration dependent structural, optical and electrochromic properties of MoO$_3$ thin films. *International Journal of Electrochemical Science* 3(8): 953-960.

Rodríguez-Paéz, J.E., Caballero, A.C., Villegas, M., Moure, C., Durán, P. & Fernández, J.F. 2001. Controlled precipitation methods:formation mechanism of ZnO nanoparticles. *Journal of the European Ceramic Society* 21(7): 925-930.

Song, J., Ni, X., Gao, L. & Zheng, H. 2007. Synthesis of metastable h-MoO$_3$ by simple chemical precipitation. *Materials Chemistry and Physics 102*(2-3): 245-248.

Ueda, W., Sadakane, M. & Ogihara, H. 2008. Nano-structuring of complex metal oxides for catalytic oxidation. *Catalysis Today* 132(1-4): 2-8.

Ungár, T. 2004. Microstructural parameters from X-ray diffraction peak broadening. *Scripta Materialia* 51(8): 777-781.

Wagner, J.B., Abd Hamid, S.B., Othman, D., Timpe, O., Knobl, S., Niemeyer, D., Su, D.S. & Schlögl, R. 2004. Nanostructuring of binary molybdenum oxide catalysts for propene oxidation. *Journal of Catalysis* 225(1): 78-85.

Wang, S., Zhang, Y., Ma, X., Wang, W., Li, X., Zhang, Z. & Qian, Y. 2005. Hydrothermal route to single crystalline α-MoO$_3$ nanobelts and hierarchical structures. *Solid State Communications* 136(5): 283-287.

Yu, J., Lei, M. & Cheng, B. 2004. Facile preparation of monodispersed calcium carbonate spherical particles via a simple precipitation reaction. *Materials Chemistry and Physics* 88(1): 1-4.

Yu, S., Sun, C.-J. & Chow, G.-M. 2007. Chemical synthesis of nanostructured particles and films. In: C.K. Carl (ed). *Nanostructured Materials (2nd ed)*: 3-46. Norwich, New York: William Andrew Publishing.

Zhang, R., Ma, J., Li, J., Jiang, Y. & Zheng, M. 2011. Effect of pH, temperature and solvent mole ratio on solubility of disodium 5'-guanylate in water + ethanol system. *Fluid Phase Equilibria* 303(1): 35-39.

Combinatorial Technology and Catalysis Research Centre (COMBICAT)
Level 3, Blok A
Institute of Postgraduate Studies, University Malaya
50603 Kuala Lumpur
Malaysia

*Corresponding author; email: d_devi10@yahoo.com